

# Shape optimization for 2D diffusive scalar transport

Marios M. Fyrillas\*

Department of Mechanical Engineering  
Frederick University Cyprus, 1303 Nicosia, Cyprus

October 23, 2008

## Abstract

A new theoretical formulation is presented for the shape optimization problem associated with maximizing or minimizing the diffusive scalar transport from a two-dimensional body. In particular, we consider the diffusive transport of heat from an isothermal body into a medium with constant temperature at the far-field. The formulation also applies to mass and momentum transport. The diffusion problem, which is governed by the Laplace equation, is addressed using conformal mapping techniques where the two-dimensional domain is mapped onto a simpler domain where an analytical solution can be readily obtained. The objective function of the optimization problem is the length of the object in the transformed domain and the variables of the optimization are the parameters of the Schwarz-Christoffel transformation. The length of the object in the transformed domain is related to the scalar displacement, which corresponds to a far-field temperature drop or rise (slip velocity in case of momentum transport), that depends on the shape of the body and it quantifies the enhancement or reduction in transport rate. The mathematical formulation is validated by addressing two fundamental shape optimization problems associated with maximizing or minimizing the transport rate (drag in case of momentum transport) from a two-dimensional body of unit span: i) for a given surface area to obtain the shape that maximizes the transport rate from a body, ii) for a given volume to obtain the shape that minimizes the transport rate from a body. For both cases we compute numerically that the cylinder is the optimal shape. The versatility of the formulation is further demonstrated by including constraints with respect to the length of the body.

## Keywords

Shape Optimization; Diffusive Transport, Heat Conduction, Shear flow; Schwarz-Christoffel transformation; Slip Velocity, Scalar Displacement; Laplace equation.

---

\*E-mail: m.fyrillas@frederick.ac.cy

# 1 Introduction

Determining the shape or surface geometry that maximizes or minimizes (extremizes) transport is of fundamental importance in many engineering applications [27, 2]. For example: obtain the optimum shape of a condenser plate [23, 17], the design of minimum seepage loss canals [16, 29], drag reduction in external flows [5], minimization of the thermal resistance of an inverted fin intruding into a conducting wall [3]. From a mathematical point view, computing the shape (iso-perimetric extremum) that extremizes the transport rate suggests a challenging problem of constrained optimization. In this work, using the Schwarz-Christoffel transformation, the problem is formulated as a nonlinear programming problem (constrained nonlinear optimization [10, 21]) i.e., find the constrained extremum of a scalar function of several variables.

The particular shape optimization problem we address in this work has not been previously investigated. We consider the shape optimization problem associated with optimizing the scalar diffusive transport from a two-dimensional body embedded into a medium with a constant temperature at the far-field. The problem, which is governed by the Laplace equation, is addressed using conformal mapping techniques [4, 26, 6, 22] and in particular the Schwarz-Christoffel transformation [8] through which the two-dimensional object is mapped onto a strip. The objective function of the optimization problem is the length of the strip in the transformed domain, which is related to the scalar displacement, and the variables of the optimization are the parameters of the Schwarz-Christoffel transformation. The shape optimization problems are addressed through numerical optimization [10, 21] which can handle complicated geometrical constraints and demonstrates that the formulation is robust, tractable and versatile.

The scalar displacement [12] corresponds to a temperature/concentration profile displacement in the case of heat/mass transport [12] or a slip velocity in the case of momentum transport [28, 19, 18, 25] and it quantifies the enhancement or reduction in transport rate [1, 20]. This claim is justified in [12], however is repeated here for ready reference: consider diffusive heat transport from a flat surface located at  $y = 0$  held at a constant temperature  $T_0$ , subject to a fixed transport rate,  $q''$ , into the infinite overlying medium. Elementary analysis shows that the temperature profile is given by  $T = T_0 + \gamma y$ , where  $\gamma = -q''/\kappa$  is the ratio of the flux  $q''$  to the medium thermal conductivity  $\kappa$ . If the surface is not perfectly flat, then, a non-linear temperature field is established ( $\tilde{T}$ ) and the temperature profile *far from the surface* is modified to obtain the form  $\tilde{T}(y \rightarrow \infty) \sim T_0 + \tilde{\gamma}y + \Delta T_D$ , where  $\Delta T_D$  represents the temperature displacement. The value of the displacement is directly related to the shape of the surface and has very significant ramifications on the transport rate. This can be justified if we replace the Neumann far-field condition with a Dirichlet boundary condition, i.e. instead of specifying the flux at the far-field we specify the temperature. Hence, we consider the problem where a planar surface held at a constant temperature  $T^\infty$  is placed at the far-field, i.e. a distance  $d$  where  $d$  is sufficiently large. For the flat surface the flux,  $\gamma$ , is equal to

$$\gamma = \frac{T^\infty - T_0}{d},$$

and for the non-flat surface the average flux,  $\tilde{\gamma}$ , is equal to

$$\tilde{\gamma} = \frac{T^\infty - (T_0 + \Delta T_D)}{d}.$$

A negative value of  $\Delta T_D$ , i.e. an effective surface temperature decrease, would constitute an enhancement in transport rate while a positive value would constitute a reduction in transport. This example illustrates how the value of  $\Delta T_D$  quantifies the effect of the surface geometry on the transport rate. Hence, an extremum of the scalar displacement is equivalent to an extremum of the net transport rate.

Motivated by the example outlined in the preceding paragraph, we consider the diffusive transport of heat from an isothermal body into an infinite medium with a constant heat transfer rate at the far-field. The governing equation is the Laplace equation with Dirichlet boundary condition over the body and constant heat flux at the far-field. Even though we consider heat transport, the analysis also applies to mass and momentum transport. With respect to momentum transport the formulation models the uni-directional, shear flow along a two dimensional body with constant shearing rate at the far-field [26, 22]. The main objective is to obtain the shape that would lead to an optimum transport rate. The physical arguments of the optimization strategy are as follows. The local transport rate is proportional to the local surface area, hence we expect that an increase in the surface area will result in a higher overall transport rate. However, the local transport rate is also proportional to the local scalar gradient which directly depends on the shape of the surface element, hence, both the area and the shape of the surface element affect the increase or decrease in the transport rate. These arguments comprise the rationale of the physics behind the optimization strategy: find the optimal shape such that the distribution of the scalar gradient on the surface contributes to an optimal overall transport rate.

In the next Section (Section §2) we formulate the problem using the conformal mapping method. In Section §2.1 we pose the shape optimization problems. Our objective is twofold: i) given the surface area of the body to find its shape such that the transport rate is maximized and ii) given the volume of the body to find its shape such that the transport rate is minimized. The former is associated with maximizing the transport rate given the perimeter length of the cross-sectional profile while the latter is associated with minimizing the transport rate given the cross-sectional area. In Section §3 we present our numerical findings and we summarize our findings in the last Section §4.

## 2 Formulation

We consider steady, homogeneous, diffusive transport from a two dimensional, symmetric, isothermal body with a constant heat transfer rate at the far-field (Figure 1). To fix ideas we will refer to heat transport. However, the analysis also applies to mass and momentum transport. With respect to momentum transport the formulation models the uni-directional, shear flow, along a two dimensional body with constant shearing rate at the far-field. The governing equation is the Laplace equation,  $\nabla^2 f = 0$ , where  $f(x, y)$  might represent the

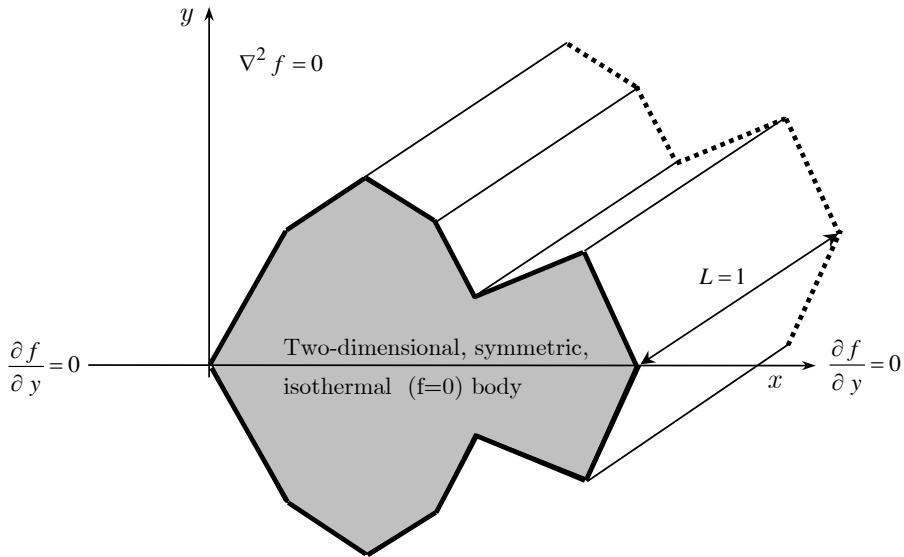


Figure 1: Schematic representation of the model problem along with boundary conditions. The field  $f$  might represent the temperature field  $T$ , or the concentration field  $C$ , or the velocity  $\mathbf{w}$  (the velocity is along the body, i.e. normal to the  $x - y$  plane). The boundary conditions are Dirichlet boundary conditions over the surface ( $f = 0$ ) and Neumann boundary condition over the rest of the  $x$ -axis. The latter is dictated by the symmetry of the body.

temperature field  $T$  (heat transport), or the concentration field  $C$  (mass transport), or the velocity  $\mathbf{w}$  (momentum transport, where  $\mathbf{w}$  is normal to the  $x, y$  plane). The constant transfer rate at the far-field implies that  $\partial f / \partial r (r \rightarrow \infty) = 1/r$ . The symmetry of the body with respect to the  $x$ -axis leads to the following boundary conditions (Figure 1); Dirichlet boundary conditions over the surface ( $f = 0$ ) and Neumann boundary condition over the rest of the  $x$ -axis ( $\partial f / \partial y = 0$ ). Here, we have non-dimensionalized the lengths with a characteristic length  $\ell$  and the scalar field  $f$  with  $q / (\kappa 2\pi L)$ , where  $q$  represents the transport rate,  $\kappa$  is the diffusion coefficient (e.g. conductivity) and  $L = 1$  (unit span).

As described by Driscoll and Trefethen [8], polygonal segments in the physical plane are mapped into a straight wall in the computational plane using the Schwarz-Christoffel transformation

$$\frac{dz}{dw} = R \prod_{j=0}^{j=N} (w - w_j)^{\alpha_j}, \quad (1)$$

where the product identifies the number of elements  $N$ . In the above transformation  $w_j$  are the images of the  $z_j$  vertices (Figure 2),  $\pi\alpha_j$  are the turning angles which are taken to be positive for the clockwise rotation,  $\alpha_0$  and  $\alpha_N$  are defined with respect to the  $x$ -axis, and  $R$  is a complex constant. For the configurations we will be considering, the  $x$ -axis is the

boundary at  $\pm\infty$  hence

$$\sum_j \alpha_j = 0. \quad (2)$$

Two points may be chosen arbitrarily. This choice is accomplished by placing the origin of the transformed domain at the origin of the physical domain and by setting the extra condition that at the far-field  $dz = dw$ , i.e.  $R = 1$ . In view of these choices and upon integration, the transformation takes the form

$$z(w; \boldsymbol{\alpha}) = \int_0^w \prod_{j=0}^{j=N} (\theta - w_j)^{\alpha_j} d\theta, \quad (3)$$

where  $\boldsymbol{\alpha}$  represents the  $N+1$ -tuple  $(\alpha_0, \alpha_1, \alpha_2, \dots, \alpha_N)$ . The difficulty of the transformation (3) is that the parameters  $w_j$  do not appear explicitly, but given the physical domain and hence the angles  $\pi\alpha_j$ , a system of non-linear equations must be solved for the unknown parameters  $w_j$ s [8]. Davis [7] also suggested that these constants can be efficiently determined through a method of successive approximations. However, in this analysis this is not necessary as we are dealing with the inverse problem, i.e. we are trying to determine the angles  $\pi\alpha_j$  while the locations of the points  $w_j$  can be preassigned.

Subsequently, the upper half of the  $w$ -plane is mapped into the upper half-strip  $-\pi/2 < u < \pi/2$  of the  $\zeta$ -plane (Figure 2) through the transformation

$$\frac{2w}{w_N} - 1 = \sin \zeta, \quad (4)$$

where  $\zeta = u + iv$ . Under this transformation (elliptical coordinates) the solution is simply  $f = v$  (see appendix A). At the far-field the temperature field behaves asymptotically as  $f(|w| \rightarrow \infty) \sim \ln(2\sqrt{2}|w|)/w_N$  (see appendix A). An analysis similar to the one outlined in the Introduction (§1) will justify that  $w_N$  is related to the scalar displacement and consequently to the enhancement or reduction in the transport rate from the body; a larger  $w_N$  constitutes enhancement while a smaller constitutes reduction. Hence, the objective function of the optimization procedure is  $w_N$ .

For reasons that will be apparent subsequently and in view of equation (2), we normalize  $z$ ,  $w$  and  $\theta$  with respect to  $w_N$

$$\hat{z}(\hat{w}; \boldsymbol{\alpha}) = \int_0^{\hat{w}} \prod_{j=0}^{j=N} (\hat{\theta} - \hat{w}_j)^{\alpha_j} d\hat{\theta}.$$

Note that the variable  $\hat{z}$  does not depend explicitly on  $w_N$ . In what follows we define  $\hat{z}_i$ , which represents the location of the normalized vertices in the physical domain, through:

$$\hat{z}_i = \hat{z}_i(\boldsymbol{\alpha}) = \hat{z}(\hat{w}_i; \boldsymbol{\alpha}) = \int_0^{\hat{w}_i} \prod_{j=0}^{j=N} (\hat{\theta} - \hat{w}_j)^{\alpha_j} d\hat{\theta} \quad (5)$$

where, as mentioned earlier, the  $\hat{w}_j$ s (and  $\hat{w}_{j,s}$ ) are preassigned; for example equispaced points ( $N+1$ -tuple) between 0 and 1.

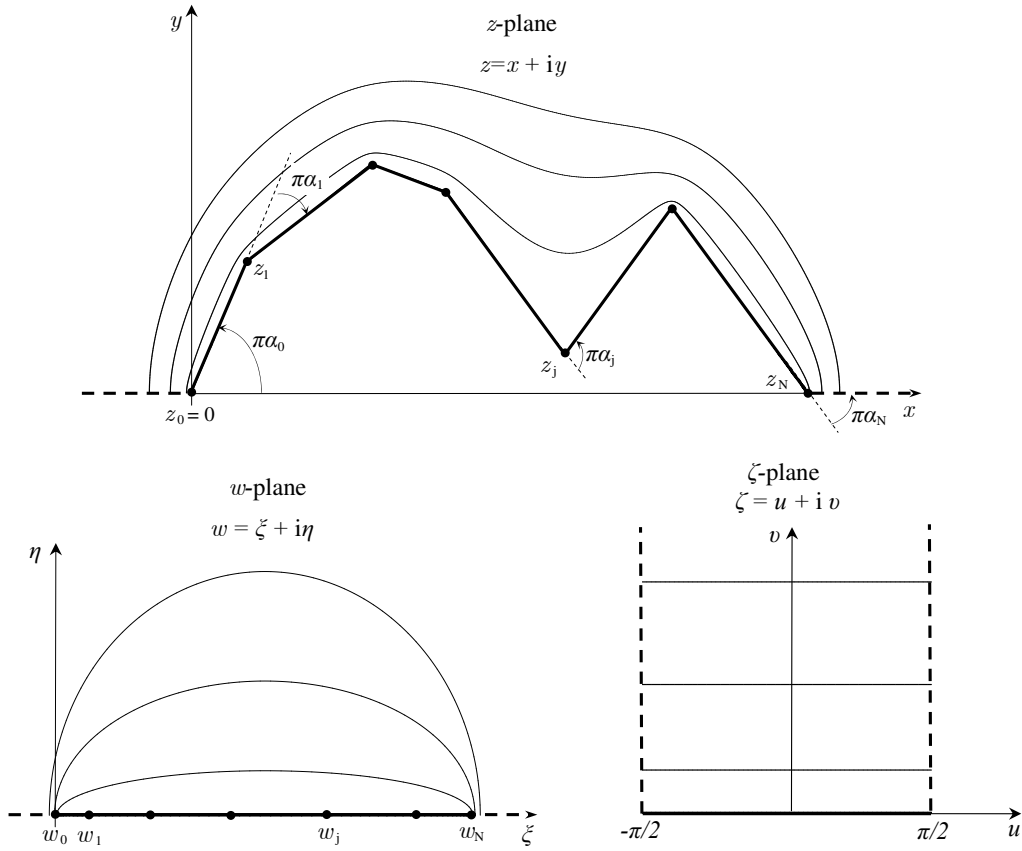


Figure 2: Mapping of a polygon in the physical  $z$ -plane into the upper half-strip  $-\pi/2 < u < \pi/2$  of the  $\zeta$ -plane. The boundary conditions are Dirichlet ( $f = 0$ ) over the body (thick solid lines) and Neumann along the symmetry line (dashed lines). Horizontal lines in the  $\zeta$ -plane are isothermal lines and the figures illustrate their transformation under the SC transformations.

## 2.1 Optimization

In what follows we develop two optimization strategies in order to extremize  $w_N$  subject to certain geometrical constraints. The constraints are necessary in order to achieve a solution because each value of  $w_N$  would correspond to an infinite number of shapes. We define  $P$  as the dimensionless perimeter, i.e. the perimeter divided by the characteristic length scale  $\ell$ , of the polygonal segments associated with the half-body

$$P(\boldsymbol{\alpha}) = w_N \sum_{i=0}^{N-1} |\hat{z}_{i+1} - \hat{z}_i|, \quad (6)$$

and the dimensionless area  $A$ , i.e. the area divided by the square of the characteristic length scale  $\ell^2$ , associated with the half-body:

$$A(\boldsymbol{\alpha}) = w_N^2 \sum_{i=0}^{N-1} \frac{\text{Im}(\hat{z}_{i+1} + \hat{z}_i)}{2} \text{Re}(\hat{z}_{i+1} - \hat{z}_i) = \frac{w_N^2}{2} \sum_{i=0}^{N-1} (\hat{y}_{i+1} + \hat{y}_i) (\hat{x}_{i+1} - \hat{x}_i). \quad (7)$$

We proceed to formulate the optimization problems with respect to  $w_N$  as justified in the previous sections. Maximizing the transport rate, given the perimeter length of the cross-sectional profile of the body, is equivalent to maximizing  $w_N$ . In view of equation (6) the problem is formulated as follows:

$$\underset{\boldsymbol{\alpha}}{\text{minimize}} \quad \sum_{i=0}^{N-1} |\hat{z}_{i+1} - \hat{z}_i| \quad (8)$$

subject to the constraints

$$\begin{aligned} \sum_i \alpha_j &= 0 \\ \text{Im}(\hat{z}_N) &= \hat{y}_N = 0. \end{aligned} \quad (9)$$

A similar approach can be employed to define an optimization problem with respect to the area. The difference is that trying to maximize transport rate for a prescribed area would lead to a shape with spikes. Therefore we pose a minimization problem with respect to the transport rate or equivalently we minimize  $w_N$  given the cross-sectional area of the body. In view of equation (7) the problem is formulated as follows:

$$\underset{\boldsymbol{\alpha}}{\text{maximize}} \quad \sum_{i=0}^{N-1} (\hat{y}_{i+1} + \hat{y}_i) (\hat{x}_{i+1} - \hat{x}_i) \quad (10)$$

subject to the constraints

$$\begin{aligned} \sum_i \alpha_i &= 0 \\ \text{Im}(\hat{z}_N) &= \hat{y}_N = 0. \end{aligned} \quad (11)$$

The geometrical constraints, as expressed through equations (9) and (11) are necessary in view of the specific problem we are addressing (see Figures 1 and 2).

### 3 Model calculations

In general, the computation of the shape (iso-perimetric extremum) that extremizes the transport rate suggests a challenging problem of constrained optimization. In this work, using conformal mapping techniques [8], the shape optimization problems (8 and 10) are formulated as nonlinear programming problems (constrained nonlinear optimization, [10, 21]), i.e. finding the constrained extremum of the scalar function of several variables  $w_N(\boldsymbol{\alpha})$ . Attempting to prove the existence of a global extremum or developing a specialized numerical technique, is beyond the scope of this work. Rather, our main objective is to address the fundamental problem of shape optimization for 2-dimensional diffusive scalar transport. Experimentation has shown that the Optimization Toolbox of MATLAB [21, 11, 14] is successful in addressing the shape optimization problems considered in this work.

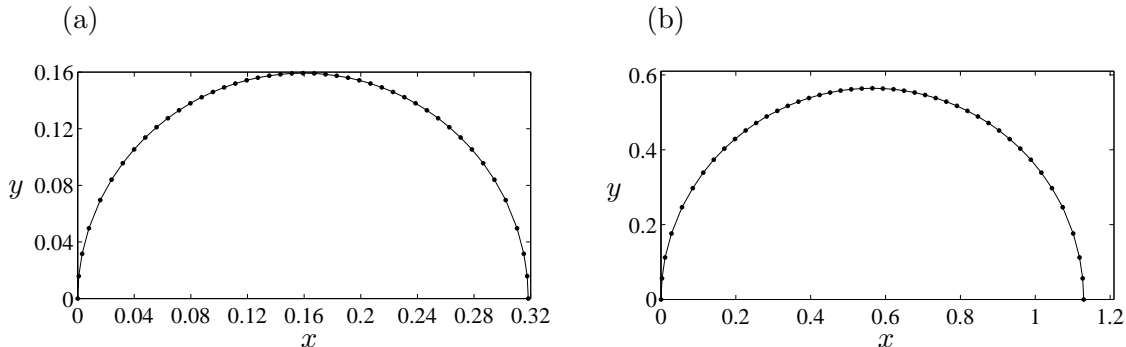


Figure 3: Optimal shapes obtained numerically using the optimization algorithm outlined in section §2.1. The points were obtained using an optimization procedure and the solid curves correspond to a semicircle. (a) Transport rate maximization given a two-dimensional body of unit perimeter length, i.e. the semicircle has a radius  $r = 1/(2\pi)$ , (b) Transport rate minimization given a two-dimensional body of unit cross-sectional area, i.e. the semicircle has a radius  $r = \sqrt{1/\pi}$ .

In our numerical optimization, both the objective function and the nonlinear constraints require the evaluation of the integral  $\hat{z}_i$  (equation 5) which has integrable power-law singularities. This is achieved through Gauss-Jacobi quadrature as outlined by Driscoll and Trefethen [8, 9]. As we have mentioned earlier, the shape optimization problem is an inverse problem in the sense that while the classical approach is to compute the  $w_i$ s for a given shape, i.e. the angles  $\alpha_i$ s are known, what is needed here is to compute the shape, i.e. both  $w_i$ s and  $\alpha_i$ s. Experimentation has shown that the shape optimization problem can be successfully addressed by choosing the  $w_i$ s and computing the  $\alpha_i$ s through optimization. Furthermore, choosing the  $w_i$ s to be equispaced proved to be adequate except near large slopes, i.e. when  $\alpha_i$ s are large, where we included some extra points in order to improve the accuracy. The computations were performed on a personal computer and converged usually within 10-20 iterations, while a complete calculation did not require more than 5-10 minutes of CPU time. Hence, we did not consider necessary to include explicit expressions for the gradient of the objective function and the constraints. As a starting vector we have used  $\alpha = 0$ , however the accuracy of the converged solution was verified by repeating the calculation with smaller tolerances and a different starting vector.

The shape optimization problems posed in the previous section are solved to obtain that the cylinder is the optimal shape (see Figures 3a and 3b) for both, the transport maximization and minimization [17] problems, which is not surprising in view of the isoperimetric theorem [24].

The optimization procedure is further employed to obtain the optimal shapes given the length of the body. Subsequently, this length is used as the characteristic length in the non-dimensionalization ( $\ell$ ), and an additional constraint is included:

$$\text{Re}(\hat{z}_N) = \hat{x}_N = \frac{1}{w_N}. \quad (12)$$

To circumvent the complication that the minimization variable (objective function)  $w_N$  now appears in the constraint we modify the numerical procedure: we assume a value for  $w_N$ , and the optimization procedure now provides the value of the dimensionless perimeter length (6) in the case of maximizing the transport rate, or the dimensionless area (7) in the case of minimizing the transport rate. This procedure suggests that maximizing the transport rate given the perimeter length of the 2D shape is equivalent to minimizing the length given the transport rate. Conversely, minimizing the transport rate given the area of the 2D shape is equivalent to maximizing the area given the transport rate.

In Figure (4a) we show the optimal curves obtained from the numerical solution of the transport maximization problem (shape optimization problem 8) with the additional constraint (12). Three different cases were investigated,  $w_N = 1.3, 2$  and  $3$ , which correspond to the bottom, middle and top curves, respectively. The solid points connected with dotted curves correspond to the  $z_j$ s obtained through numerical optimization. For values of  $w_N < 2$  the optimal curves resemble arcs of circles shown on the bottom curve of Figure (4a). When  $w_N = 2$  we obtain a semi-circular shape (Figure 4a middle curve); this value can be verified using the Joukowski transformation. For values of  $w_N > 2$ , the optimization produces shapes beyond the allowable length, consequently we have to include the extra constraint  $0 \leq \hat{x}_i \leq 1/w_N$ . The optimal shapes (Figure 4a top curve) have vertical sides with a semielliptical-like top.

In Figure (4b) we show the optimal curves obtained from the numerical solution of the transport minimization problem (shape optimization problem 10) with the additional constraint (12). Similar to Figure (4a), we have used the following values for  $w_N = 1.3, 2$  and  $3$ , which correspond to the bottom, middle and top curves, respectively. For values of  $w_N < 2$  we have to include the extra constraint  $\hat{y}_i > 0$  as the optimization produces non-realistic results. In this range, i.e.  $w_N < 2$ , the optimal shapes (Figure 4b bottom curve) have flat edges and attain higher values than the respective maximal transport shapes (Figure 4a bottom curve). For  $w_N = 2$ , as expected, we obtain a semi-circular shape (middle curve). For values  $w_N > 2$  the optimization produces shapes beyond the allowable length consequently we have to include the extra constraint  $0 \leq \hat{x}_i \leq 1/w_N$ . Similar to the maximization problem (Figure 4b top curve), the optimal shape has vertical sides however it is flatter.

The results demonstrate that the formulation is robust, tractable and versatile. The success of the technique relies on the conformal mapping through which the problem complexity is transferred to the mapping function. It can be successfully applied to bounded domains [13], periodic domains and problems with more complicated boundary conditions.

## 4 Conclusions

We have addressed the shape optimization problem associated with diffusive transport of heat from a two-dimensional, symmetric body embedded in a medium with a constant temperature at the far-field. The analysis also applies to mass and momentum transport. The objective is to obtain the shape that extremizes the transport rate. The objective

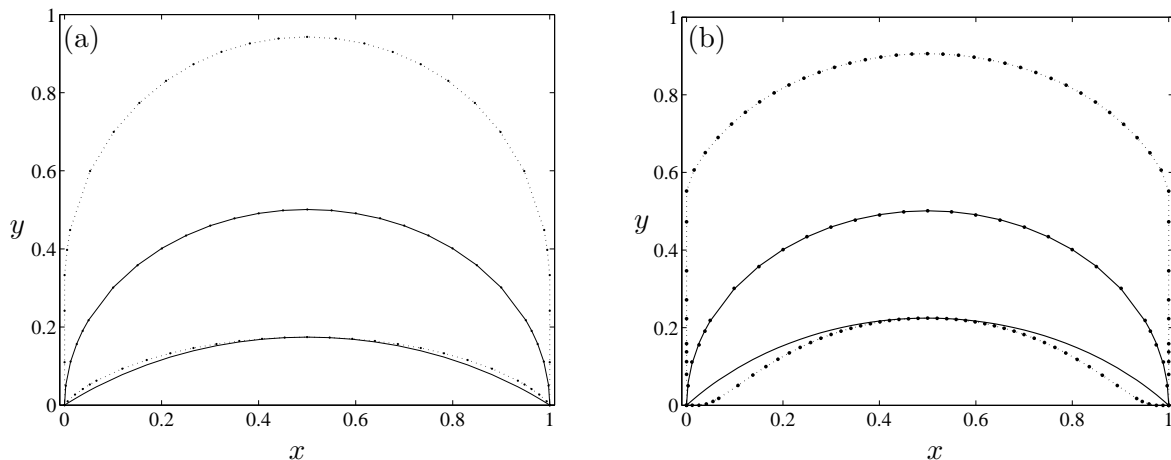


Figure 4: Optimal curves associated with maximizing (Figure a) or minimizing (Figure b) the transport rate with the additional constraint that the length of the body would not exceed a certain value. The optimal curves, for both maximization and minimization problems, coincide for  $w_N = 1$  (a straight line from the origin to the point  $(0,1)$ ), and for  $w_N = 2$  (a semi-circle, middle curves). In the figures we show results for  $w_N = 1.3$  (bottom curves) and  $w_N = 3$  (top curves). The points connected with dotted curves correspond to the numerical results while the solid curves to arcs of circles.

function, of the shape optimization procedure, is the scalar displacement which amounts to a macroscopic temperature drop or rise (slip velocity in the case of momentum transport) that depends on the geometry of the body and quantifies the enhancement or reduction in transport associated with a particular shape.

In order to obtain an expression for the scalar displacement we consider the problem of heat conduction from an isothermal body, into an infinite medium, due to a constant heat transfer rate at the far-field. With respect to momentum transport the formulation models the uni-directional, shear flow, along a two dimensional body with constant shearing rate at the far-field. Using the Schwarz-Christoffel transformation the body is mapped onto a strip where the Laplace equation has an analytical solution. The length of the strip in the transformed domain is identified to be related to the scalar displacement and is used as the objective function in the optimization problem, and the variables of the optimization are the parameters of the Schwarz-Christoffel transformation. The shape optimization problem is addressed numerically and validated by addressing two fundamental problems: i) given the perimeter length of a two-dimensional surface, to obtain the shape that maximizes transport rate and ii) given the cross-sectional area of a two-dimensional surface to obtain the shape that minimizes the transport rate. In both cases, we have obtained that the cylinder (circle) is the optimal shape. The formulation was supplemented with an additional geometrical constraint in order to include limitations with respect to the length of the body. The numerical results demonstrate the versatility and the robustness of the formulation,

which can be complicated geometrical constraints. The success of the technique relies on finding an appropriate conformal map such that the solution of the Laplace equation in the transformed domain is easier to obtain; analytically or numerically. We believe it can be successfully applied to bounded domains, periodic domains and problems with more complicated boundary conditions.

The physical arguments of the optimization strategy are as follows. The local transport rate is proportional to the local surface area, hence we expect that an increase in the surface area will result in a higher overall transport rate. However, the local transport rate is also proportional to the local scalar gradient which directly depends on the shape of the surface element, hence, both the area and the shape of the surface element affect the increase or decrease in the transport rate. These arguments comprise the rationale of the physics behind the optimization strategy: i) given the perimeter length of the cross-sectional profile of a two-dimensional body, find the optimal shape such that the distribution of the scalar gradient on the surface contributes to maximal overall transport rate, ii) given the cross-sectional area of a two-dimensional body, find the optimal shape such that the distribution of the scalar gradient on the surface contributes to minimum overall transport rate.

**Acknowledgment.** The work was initially funded by the European Research Consortium in Informatics and Mathematics (ERCIM fellowship grant 2002-06) and by the Swiss National Foundation (Research project PAER2-101107). I would like to thank Erricos Kontoghiorghes and Bernard Philippe for their support, and Costas Sophocleous, Jennifer Waterton and Keiko Nomura for their contribution.

## A Appendix: Solution in elliptical coordinates

The transformation between the  $w$ -plane and the  $\zeta$ -plane (equation 4) can be expanded in real and imaginary parts as follows

$$\frac{2(\xi + i\eta)}{w_N} - 1 = \sin(u + iv),$$

to obtain:

$$\frac{2\xi}{w_N} - 1 = \cosh v \sin u, \quad \frac{2\eta}{w_N} = \sinh v \cos u.$$

At the far-field, i.e. large  $v$ , above expressions simplify to:

$$\xi \sim \frac{w_N}{4} \exp v \sin u, \quad \eta \sim \frac{w_N}{4} \exp v \cos u.$$

In addition,  $z \sim w$  at the far-field in view of equation (3) hence,

$$|z| = r \sim |w| = \sqrt{\xi^2 + \eta^2} \sim \frac{w_N}{\sqrt{8}} \exp v.$$

From the above asymptotic expression we obtain the following approximations at the far field:

$$v \sim \ln \frac{\sqrt{8} r}{w_N}, \quad \text{hence} \quad \frac{\partial}{\partial r} \sim \frac{\partial}{\partial v} \frac{\partial v}{\partial r} = \frac{1}{r} \frac{\partial}{\partial v}.$$

The solution that satisfies the boundary conditions is simply  $f = v$ .

## References

- [1] D. W. Bechert & M. Bartenwerfer The viscous flow on surfaces with longitudinal ribs, *J. Fluid Mech.* **206** 105 (1989).
- [2] A. Bejan, *Shape and Structure, from Engineering to Nature* (Cambridge University Press, Cambridge, UK, 2000).
- [3] C. Biserni, L. A. O. Rocha and A. Bejan, Inverted fins: geometric optimization of the intrusion into a conducting wall, *Int. J. Heat Mass Transfer* **47**, 2577 (2004).
- [4] H. S. Carslaw and J. C. Jaeger, *Conduction of heat in solids* (Clarendon Press, 1959).
- [5] K. S. Choi, K. K. Prasad and T. V. Truong, *Emerging Techniques in Drag Reduction* (Mechanical Eng. Publ., London, 1996).
- [6] I. G. Currie, *Fundamental Mechanics of Fluids* (McGraw-Hill, 1974).
- [7] R. T. Davis, Numerical methods for coordinate generation based on Schwarz-Christoffel transformation, AIAA Paper No. 79-1463, 4th Computational Fluid Dynamics Conference 180 (1979).
- [8] T. A. Driscoll and L. N. Trefethen, *Schwarz-Christoffel Mapping* (Cambridge University Press, 2002).
- [9] T. A. Driscoll, *Schwarz-Christoffel Toolbox Users Guide*.
- [10] R. Fletcher, *Practical Methods of Optimization* (John Wiley and Sons, 1987).
- [11] R. Fletcher and M. J. D. Powell, A rapidly convergent descent method for minimization, *Computer Journal* **6**, 163 (1963).
- [12] M. M. Fyrillas and C. Pozrikidis, Conductive heat transport across rough surfaces and interfaces between two conforming media, *Int. J. Heat Mass Transfer* **44**, 1789 (2001).
- [13] M. M. Fyrillas, Heat conduction in a solid slab embedded with a pipe of general cross-section: Shape Factor and Shape Optimization, *Int. J. Eng. Sci.* **46**, 907 (2008).
- [14] D. Goldfarb, A family of variable metric updates derived by variational means, *Mathematics of computing* **24**, 23 (1970).
- [15] M. D. Greenberg, *Foundations of Applied Mathematics* (Prentice-Hall Inc., 1978).
- [16] A. R. Kacimov, Analytical solution and shape optimization for groundwater flow through a leaky porous trough subjacent to an aquifer. *Proc. R. Soc. Lond. A*, **462**, 1409 (2006).

- [17] A. Kacimov, Optimal shape of variable condenser. Proc. R. Soc. Lond. A, **457**, 485 (2001).
- [18] E. Lauga and H. A. Stone, Effective slip in pressure-driven Stokes flow, J. Fluid Mech. **489**, 55 (2003).
- [19] N. Lecoq, R. Anthore, B. Cichoki, P. Szymczak and F. Feuillebois, Drag force on a sphere moving towards a corrugated wall, J. Fluid Mech. **513**, 247 (2004).
- [20] P. Luchini, F. Manzo and A. Pozzi, Resistance of a grooved surface to parallel flow and cross-flow, J. Fluid Mech. **513**, 247 (2004).
- [21] *Optimization Toolbox*, The MathWorks Inc., 2000.
- [22] L. M. Milne-Thomson, *Theoretical Hydrodynamics* (New York: Dover, 1986).
- [23] P. M. Morse and H. Feshbach *Methods of Theoretical Physics, Part II*, McGraw-Hill Science/Engineering/Math, 1953.
- [24] R. Osserman, *A Survey of Minimal Surfaces* (New York: Dover, 1986).
- [25] D. Owen and B. S. Bhatt, On flow through porous material using a generalized Schwarz-Christoffel theory, Physics of fluids **71**, 3174 (1992).
- [26] R. L. Panton, *Incompressible Flow* (John Wiley & Sons, 1984).
- [27] O. Pironneau, *Optimal shape design for elliptic systems* (Springer, New York, 1984).
- [28] S. Richardson, A model for the boundary condition of a porous material: Part 2, J. Fluid Mech. **49**, 327 (1971).
- [29] P. K. Swamee, G. C. Mishra and B. R. Chahar, Design of minimum seepage loss canal sections with drainage layer at Shallow depth, J. Irrig. and Drain. Engrg., ASCE, **127**, 287 (2001).